0026-895X/11/8004-673–682$25.00
MOLECULAR PHARMACOLOGY
Vol. 80, No. 4
71381/3720786
Mol Pharmacol 80:673–682, 2011
Printed in U.S.A.

MOL PHARM
MOLECULAR PHARMACOLOGY

Aryl Hydrocarbon Receptor Activation in Hematopoietic Stem/Progenitor Cells Alters Cell Function and Pathway-Specific Gene Modulation Reflecting Changes in Cellular Trafficking and Migration[S]

Fanny L. Casado, Kameshwar P. Singh, and Thomas A. Gasiewicz

Department of Environmental Medicine, University of Rochester Medical Center, Rochester, New York

Received January 25, 2011; accepted July 26, 2011

ABSTRACT

The aryl hydrocarbon receptor (AhR) is a transcription factor belonging to the Per-ARNT-Sim family of proteins. These proteins sense molecules and stimuli from the cellular/tissue environment and initiate signaling cascades to elicit appropriate cellular responses. Recent literature reports suggest an important function of AhR in hematopoietic stem cell (HSC) biology. However, the molecular mechanisms by which AhR signaling regulates HSC functions are unknown. In previous studies, we and others reported that treatment of mice with the AhR agonist 2,3,7,8-tetrachlorodibenzo-*p*-dioxin (TCDD) compromises the competitive reconstitution of bone marrow (BM) cells into irradiated host animals. Additional studies indicated a requirement for AhR in hematopoietic cells and not marrow microenvironment cells. In this study, we tested the hypothesis that TCDD-mediated phenotypic and functional changes of HSCs are a result of changes in gene expression that disrupt stem cell numbers and/or their migration. TCDD treatment to mice increased the numbers of phenotypically defined HSCs in BM. These cells showed compromised migration to the BM in vivo and to the chemokine CXCL12 in vitro, as well as increased expression of the leukemia-associated receptors CD184 (CXCR4) and CD44. Gene expression profiles at 6 and 12 h after exposure were consistent with the phenotypic and functional changes observed. The expressions of *Scin*, *Nqo1*, *Flnb*, *Mmp8*, *Ilf9*, and *Slamf7* were consistently altered. TCDD also disrupted expression of other genes involved in hematological system development and function including *Fos*, *JunB*, *Egr1*, *Ptgs2* (*Cox2*), and *Cxcl2.* These data support a molecular mechanism for an AhR ligand to disrupt the homeostatic cell signaling of HSCs that may promote altered HSC function.

Introduction

The aryl hydrocarbon receptor (AhR) is a basic helix-loop-helix protein belonging to the Per-ARNT-Sim superfamily of proteins. Many of the Per-ARNT-Sim proteins sense molecules and stimuli from the cellular/tissue environment and initiate signaling cascades to elicit appropriate cellular responses. Lipophilic compounds such as halogenated and polycyclic aromatic hydrocarbons, including the potent exogenous ligand 2,3,7,8-tetrachlorodibenzo-*p*-dioxin (TCDD) (Poland and Glover 1973), bind to the cytoplasmic AhR, leading to a sequence of conformational changes that ultimately transform the AhR into its high-affinity DNA binding form in the nucleus to function as a transcription factor (Soshilov and Denison 2008).

Epidemiological data have correlated accidental and occupational exposure to TCDD and related dioxins with increased risk for certain hematological diseases such as non-Hodgkin's lymphoma, chronic lymphocytic leukemia, and multiple myeloma in humans (Frumkin, 2003). In addition, there is much data indicating that persistent activation of AhRs results in immunosuppression in different animal models (Stevens et al., 2009). AhR-dependent thymic atrophy, a hallmark of exposure to varying doses of TCDD, may be elicited by different mechanisms including 1) reduced seed-

This work was funded by the National Institutes of Health National Institute of Environmental Health Sciences [Grants ES01247, ES07026, ES04862, ES016606].

Article, publication date, and citation information can be found at http://molpharm.aspetjournals.org.

doi:10.1124/mol.111.071381.

[S] The online version of this article (available at http://molpharm.aspetjournals.org) contains supplemental material.

ABBREVIATIONS: AhR, aryl hydrocarbon receptor; TCDD, 2,3,7,8-tetrachlorodibenzo-*p*-dioxin; BM, bone marrow; HSC, hematopoietic stem cell; URMC, University of Rochester Medical Center; 7AAD, 7-amino-actinomycin D; LSK, lineage-depleted, Sca-1$^+$ and c-kit$^+$; APC, allophycocyanin; FITC, fluorescein isothiocyanate; IL, interleukin; PBS, phosphate-buffered saline; CXCL12, chemokine (C-X-C motif) ligand 12; PE, phycoerythrin; RT^2, real-time reverse transcription; PCR, polymerase chain reaction; IPA, Ingenuity Pathway Analysis; ANOVA, analysis of variance; SLAM, signaling lymphocyte activation molecule; NF-κB, nuclear factor-κB.

ing of the thymus by bone marrow (BM)-derived progenitors (Fine et al., 1990), 2) reduced stromal-mediated proliferation of thymocytes (Kremer et al., 1994; Frericks et al., 2007), and 3) a skewing of the thymic output through direct effects on developing thymocytes (Laiosa et al., 2010). In addition, AhR activation leads to 1) alterations of B lineage cells during gestation with possible consequences on autoimmunity (Mustafa et al., 2008), 2) decreased numbers of immature B cells (Murante and Gasiewicz, 2000), and 3) altered functional activity of early hematopoietic progenitors (Murante and Gasiewicz, 2000; Sakai et al., 2003; Singh et al., 2009). A single dose of TCDD that results in BM TCDD concentrations of <1 nM (Fine et al., 1990) increases the relative numbers of phenotypically defined HSCs/progenitors (Staples et al., 1998) starting 2 days after treatment and lasting until day 31 (Murante and Gasiewicz, 2000). Furthermore, TCDD-treated phenotypically defined long-term HSCs were unable to sustain peripheral blood repopulation (Sakai et al., 2003) and had a compromised ability to competitively repopulate the BM of irradiated mice (Singh et al., 2009). These effects were dependent on the presence of the AhR in hematopoietic cells but not on supporting stroma (Staples et al., 1998; Sakai et al., 2003). Taken Together, these data support a hypothesis that primitive progenitors of hematopoiesis in the BM are targeted by AhR ligands, resulting in AhR-mediated phenotypic and functional changes. Given recent interest in the possible use of AhR ligands for the expansion of HSCs and their use in BM transplants (Boitano et al., 2010), as well as in treatment of autoimmune disease (Quintana et al., 2010), it is critical to further define mechanisms related to effects on hematopoietic cell function and the signaling pathways that may mediate these alterations.

This work tests the hypothesis that TCDD- and AhR-mediated phenotypic and functional changes of murine HSCs are a consequence of disruption of stem cell numbers and/or their migration is preceded by changes in gene expression. Understanding these changes in gene expression and their functional consequences in HSCs may provide a rationale to define a role of AhR in HSCs. Furthermore, this information may provide avenues to further explore the use of therapeutic AhR ligands.

Materials and Methods

Mice and Treatments. Five-week-old C57BL/6J female mice were purchased from The Jackson Laboratory (Bar Harbor, ME) and housed in the facilities of the University of Rochester Medical Center (URMC) (Singh et al., 2009) for at least 1 week before treatment. CD45.1$^+$ (B6.SJL-Ptprc(a)/BoAiTac) female mice used in repopulation experiments were purchased from Taconic Farms (Germantown, NY).

TCDD was obtained from Cambridge Isotopes (Andover, MA), and 6-μg/ml aliquots were prepared as described previously (Laiosa et al., 2010). Either 30 μg of TCDD in olive oil/kg b.wt. or olive oil alone in a volume of 0.1 ml/20 g b.wt. was given orally by gavage. Mice were euthanized after 7 days for functional and phenotypic experiments. This dose and time were chosen on the basis of the optimal effects of TCDD on HSCs (Singh et al., 2009). To study gene expression, treated mice were euthanized 6 and 12 h after treatment.

Cell Preparations. BM was harvested from femurs and tibias, red blood cells were lysed, and lineage-positive leukocytes were depleted as described previously (Singh et al., 2009). Only cell suspensions with viability >95% as measured by exclusion of trypan blue were used for further experimentation. All flow cytometric analyses and separations were performed on viable populations only, as measured by exclusion of the fluorescent dye 7-amino-actinomycin D (7AAD). Lineage-depleted Sca-1$^+$ and c-kit$^+$ (LSK) cells used in microarray experiments were obtained by laser-assisted sorting of lineage-depleted cells stained with fluorochrome-conjugated antibodies against Sca-1$^+$ [D7, allophycocyanin (APC); ebioscience, San Diego, CA] and c-kit$^+$ [2B8, fluorescein isothiocyanate (FITC); BD Pharmingen, San Diego, CA] using a FACSAria cell sorter (BD Biosciences, San Jose, CA) and a gating scheme published recently (Singh et al., 2010). To examine differentiation of LSK cells under conditions in vitro, LSK cells were obtained from mice treated with TCDD (30 μg/kg, 7 days) or vehicle. In 12-well plates, 3×10^4 cells (10^4 cells/ml) were cultured per well. Each well contained StemSpan Serum-Free Expansion Media (STEMCELL Technologies, Vancouver, BC, Canada) supplemented with IL-6 (50 ng/ml) or IL-6 plus stem cell factor (100 ng/ml). Cells were harvested after 7 or 14 days, and phenotypic characterization was performed by flow cytometry.

Determination of Competitive Repopulation Units. The engraftment and proportion of competitive repopulation units, per million of donor's BM cells injected into the irradiated recipients, were calculated for short-term and long-term reconstitutions (6 and 20 weeks after transplantation, respectively). A limiting-dilution approach was used for quantification. BM cells were isolated from control or TCDD-treated mice. The donor's (CD45.2$^+$) cells were resuspended in 100 μl of PBS at three concentrations (0.1, 0.2, and 1×10^6) and mixed with 100 μl of PBS containing 2×10^5 competitive donor's (CD45.1$^+$) BM cells. Recipient (CD45.1$^+$) mice were irradiated with two doses of 5.5 Gy from a cesium source. Mixtures of donor and competitive donor cells were injected intravenously in eight recipients. After 6 (short-term) or 20 (long-term) weeks after transplantation, recipients were sacrificed, and BM cells were isolated. BM cells were stained using commercially fluorochrome-conjugated antibodies against CD45.1 (A20, APC; BD Pharmingen) and CD45.2 (104, FITC; BD Pharmingen) and analyzed using a FACSCanto (BD Biosciences) flow cytometer. Engraftment of the progeny was evaluated on the basis of the percentages of donor-derived CD45.2$^+$ BM cells. For the limiting-dilution analysis, the presence of more than 1% cells of donor origin (Cd45.2$^+$) was considered as positive engraftment. The proportions of HSCs per million BM cells were calculated, assuming single-hit Poisson statistics (Purton and Scadden, 2007) and using L-Calc software (STEMCELL Technologies).

Migration of Hematopoietic Precursors. The in vivo migration of hematopoietic precursors was examined 24 h after intravenous injection. An injection of 250 μl of sterile PBS containing 5 million TCDD- or vehicle-treated donor BM cells was given in the tail vein of nonirradiated recipients. The number of BM cells used was optimized experimentally and represents approximately 6.3% of the total number of BM cells in wild-type mice (i.e., recipients). The migration of phenotypically defined HSCs/progenitors was calculated as the ratio of the numbers of CD45.2$^+$ LSK cells retrieved from transplanted recipients per the numbers of CD45.2$^+$ donor LSK cells injected.

The in vitro migration was studied with a transwell assay. To each well of a V-bottom 96-well plate (BD, Franklin Lakes, NJ),150 μl of the chemoattractant murine chemokine (C-X-C motif) ligand 12 (CXCL12), also known as stromal-derived factor-1α (Miltenyi Biotech, Bergisch Gladbach, Germany), was added at concentrations of 0, 50, 100, or 300 ng/ml. The HTS Transwell 96 Permeable support with a 5-μm polycarbonate membrane (Corning Life Sciences, Lowell, MA) was placed on top of the plate containing chemoattractant. Then 500,000 lineage-depleted (Lin$^-$) cells resuspended in 50 μl of PBS were placed on top of the permeable support and incubated at 37°C for 3 h at 5% CO_2. To determine migration, cells that were recovered from the bottom well were stained with 7AAD and fluorochrome-conjugated antibodies against Sca-1 and c-kit.

Phenotyping of Cells. Flow cytometry was performed using a LSR-II flow cytometer (BD Biosciences) in the Flow Core Facility of

the URMC and was used to phenotypically define long-term and short-term HSCs (Kiel et al., 2005) using fluorochrome-conjugated antibodies against CD48 [HM48-1, phycoerythrin (PE)-Cy7; BD Pharmingen] and CD150 (9D1, APC; ebioscience). LSK cells [Sca-1 (E13-161.7, APC; BD Pharmingen) and c-kit (2B8, PE-Cy5; BD Pharmingen)] were phenotyped for the expression of markers involved in the interactions between HSCs and their microenvironment such as the integrin dimer $\alpha4\beta1$ (also known as very late antigen-4) composed of CD49d (also known as $\alpha4$; R1-2, PE; BD Pharmingen) and CD29 (also known as $\beta1$; Ha2/5, FITC; BD Pharmingen), CD184 (2B11/CXCR4, APC; BD Pharmingen), CD44 (IM7, PE-Cy5; BD Pharmingen), and CD162 (also known as P-selectin glycoprotein ligand-1; 2PH1, PE, BD Pharmingen). Flow cytometric analysis was performed in viable cells excluding 7AAD. For apoptosis analysis, Lin^- cells were incubated with fluorochrome-conjugated antibodies against c-kit (2B8, APC) and Sca-1 (D7, V450). Cells were washed and resuspended in 1× Annexin V binding buffer (BD Pharmingen) and then incubated with 7AAD and Annexin V-PE according to the manufacturer's recommendations. 7AAD and Annexin V double-negative cells were gated as viable cells, and 7AAD-negative and Annexin V-positive cells were gated as apoptotic cells. Unstained, single fluorochrome and all-fluorochromes-except-one were used to compensate for the fluorescent signals. Data were calculated and plotted using FlowJo software (Tree Star Inc., Ashland, OR).

Microarray Experiments. Total RNA was isolated from sorted LSK cells pooled from 20 mice using an RNeasy Mini/Micro Kit (QIAGEN, Valencia, CA), DNase-treated, and quantified using the ND-1000 spectrophotometer (NanoDrop Technologies, Wilmington, DE). Microarray analyses were done according to standard operating procedures by the Functional Genomics Center at the URMC. RNA quality was confirmed by the presence of two peaks on a 2:1 ratio of intensity of 28S:18S rRNA using an Agilent 2100 Bioanalyzer (Agilent Technologies, Santa Clara, CA). RNA (20 ng) was amplified using the NuGEN Ovation RNA Amplification System (NuGEN Technologies Inc., San Carlos, CA) to yield single-stranded cDNA and then were hybridized with the GeneChip Mouse Gene 1.0 ST Array (Affymetrix, Santa Clara, CA). Five microarrays from independent RNA preparations per treatment were used. The microarrays were processed as described previously (Henry et al., 2010). The relative fold changes of the signal intensity averages of TCDD with respect to the control at the 6- and 12-h time points were calculated for each of the 35,556 probes. Assuming a normal distribution of the data, we performed an F-test to evaluate variances between the treated and control groups and to calculate the p value obtained after a two-tailed Student's t test using Microsoft Excel.

Gene-Specific Primers and Real-Time Reverse Transcription. Gene-specific primers and RT^2-PCR analysis were used to validate microarray data using a set of genes selected because of their significant fold change expression differences at 6 and/or 12 h. First-strand cDNA was prepared from 100 ng of total RNA following the protocol for the SuperScript II First Strand cDNA Synthesis system (Invitrogen, Carlsbad, CA). After selecting a panel of genes of interest (Supplemental Table 1), RT^2-PCR was performed using protocols provided by the commercial provider of primers and master mix (SA Biosciences, Frederick, MD) in an iCycler System (Bio-Rad Laboratories, Hercules, CA). Fold changes in expression of genes from TCDD-treated LSK cells were calculated with respect to vehicle-treated LSK cells using the $2^{-\Delta\Delta C_t}$ approximation method. *Gapdh* and *Hprt1* were used as control endogenous genes to normalize gene expression. A linear regression coefficient close to 1 was used to assess validation of microarray data with RT^2-PCR.

Gene Expression Analysis. Transcripts with a fold change expression (TCDD normalized expression/vehicle normalized expression) greater than 1.5 at each time point were filtered. The most variable transcripts were visualized using the open-source software TIGR Multi-experiment Viewer (version 4.6.1) (Saeed et al., 2003). Relevant functional association networks were generated by Ingenuity Pathway Analysis (IPA) software (version 8.7; Ingenuity Systems, Redwood City, CA). For this purpose, the data sets containing all gene identifiers and corresponding fold change expression values were uploaded into the application. Each identifier was mapped to its corresponding object in Ingenuity's Knowledge Base. A cutoff of 1.5-fold change was set to identify transcripts whose expression was regulated. Transcripts with altered expression were overlaid onto a global molecular network developed from information contained in Ingenuity's Knowledge Base.

Statistical Analyses. Unless otherwise specified, results were analyzed and plotted using GraphPad Prism (version 5.03; GraphPad Software Inc., La Jolla, CA). The p value from a Pearson χ^2 test for goodness of fit to a binomial distribution ($p = 1$) was used to analyze the competitive repopulation unit data. When appropriate, a two-tailed Student's t test and two-way ANOVA were used to analyze statistical significance. $p < 0.05$ was considered to be statistically significant. A right-tailed Fisher exact test was used to calculate a p value to determine the probability that each biological function and/or disease assigned to that data set by IPA is due to chance alone.

Results

AhR Activation by TCDD Alters Phenotype and Functions of HSCs. Our laboratory and others have consistently observed alterations of phenotypically defined HSCs/progenitors after TCDD treatment (Murante and Gasiewicz, 2000; Sakai et al., 2003; Singh et al., 2009). In this study, we asked questions about the relative expression of newly recognized phenotypes of HSCs (Kiel et al., 2005) as well as qualitative and quantitative functional characteristics of BM cells. Seven days after in vivo treatment with TCDD, populations of HSCs were analyzed using flow cytometry based on their relative expression of the signaling lymphocyte activation molecule (SLAM) receptors (Wilson et al., 2008) as phenotypic markers of BM stem cells. Figure 1A shows that representative gating applied to all samples used to determine the relative percentages of LSK, $LSKCD48^-CD150^-$, and $LSKCD48^-CD150^+$ populations. As observed previously (Murante and Gasiewicz, 2000; Singh et al., 2009), TCDD treatment resulted in a significant increase in the relative percentage of LSK cells (Fig. 1B). However, only a small proportion of the LSK population is made up of those cells defined as HSCs, with the largest subpopulation being composed of predominantly more mature multipotent progenitor cells. As such, it is notable that TCDD also increased the relative percentages of the subpopulations $LSKCD48^-CD150^-$ and $LSKCD48^-CD150^+$, which have been correlated with short-term HSCs and multipotent progenitor and long-term HSCs, respectively (Fig. 1C).

To characterize the functional quality of HSCs, the progeny of short-term and long-term HSC donor cells was analyzed after 6 or 20 weeks of competitive repopulation, respectively. Hematopoietic cells from a donor or competitive donor origin were distinguished using flow cytometry (Fig. 2, A–C). Under the experimental conditions used, no differences between TCDD and vehicle were observed 6 (Fig. 2D) or 20 (Fig. 2E) weeks after transplantation. The proportions of short- and long-term HSCs per million BM cells (Table 1) were calculated from limiting dilution analysis to characterize quantitatively the functional integrity of these cells. By this analysis, the numbers of competitive functional HSCs from TCDD-treated animals were not significantly different from those from vehicle controls. To complement this analysis, we

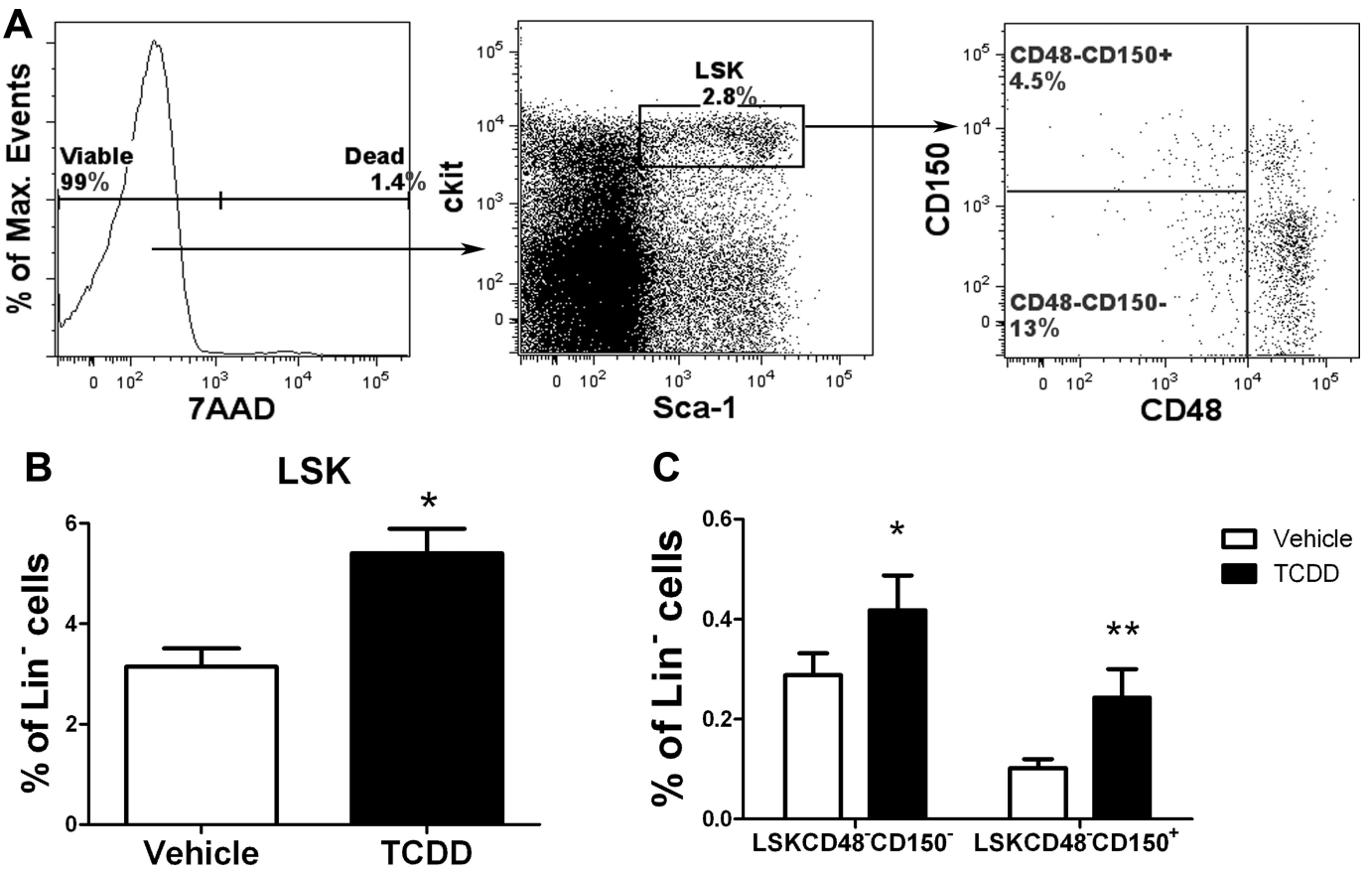

Fig. 1. TCDD treatment altered phenotypically defined HSC populations. Lin$^-$ cells were harvested from mice treated with TCDD (30 μg/kg, 7 days) or vehicle. Flow cytometry was used to phenotypically characterize populations of HSCs. A, dead cells were excluded and the LSK cell population was gated from the viable cells. From the LSK population, further gating was applied on the basis of CD48 and CD150. Cumulative data for the percentages of the HSC-enriched population are indicated. LSK cells ($p = 0.0059$) (B) and subpopulations LSKCD48$^-$CD150$^-$ ($p = 0.0075$) and LSKCD48$^-$CD150$^+$ ($p = 0.0007$) (C) in Lin$^-$ cells. Error bars are S.E.M. for $n = 3$ independent experiments using data from five to six individual mice. *, $p < 0.05$; **, $p < 0.001$.

evaluated the ability of LSK cells from TCDD-treated mice to undergo expansion and differentiation under ex vivo conditions. Supplemental Fig. 1 shows that, in the presence of IL-6 ± stem cell factor, TCDD-treated LSK cells are as able to grow and generate different Lin$^-$ and Lin$^+$ populations in vitro similarly to vehicle-treated LSK cells. In addition, LSK cells from TCDD-treated mice did not show any difference in the level of apoptosis as measured by Annexin and 7AAD staining (Supplemental Fig. 2). These results suggested that the TCDD dosing paradigm used to activate the AhR elicited phenotypic changes but did not alter the absolute proportions of functional HSCs when measured independently from their correlated phenotype. In addition, there were no alterations in their ability to survive, expand, and differentiate under ex vivo conditions.

TCDD Affects Migration of LSK cells. TCDD-treated LSK cells were reported to have decreased engraftment (Sakai et al., 2003; Singh et al., 2009). However, TCDD treatment elicited no difference in the overall proportions of functional HSCs independent of their phenotype (Table 1). Therefore, we hypothesized that critical events during engraftment such as the trafficking behavior of LSK cells may be affected. Figure 3A shows that migration of LSK cells from TCDD-treated animals to BM of recipients is decreased when measured as in vivo accumulation of cells to the BM after 24 h of transplantation. As a complement to this study, we also observed that the directional migration of TCDD-treated LSK cells through a semipermeable membrane to a chamber containing the chemokine CXCL12 was decreased (Fig. 3B).

The best studied receptor of CXCL12 is CD184 (CXCR4) (Sasaki et al., 2009). As such, we analyzed LSK cells for the expression of CD184/CXCR4 as well as other molecules known to participate in the interactions between HSCs and their microenvironment such as CD44, which is a receptor for osteopontin present in the extracellular matrix of the endosteum. Within the LSK population from TCDD-treated animals, there was increased mean fluorescent intensity for CD184/CXCR4 and CD44 (Fig. 3, C and D). Together these results support the fact that AhR activation leads to cell signaling-mediated disruptions in the ability of LSK cells to interact with molecules present in their microenvironment.

TCDD Alters Pathways Involved in Cell Signaling, Cellular Movement, and Cancer. The above data suggest that the previously observed TCDD-elicited changes in HSC/progenitor engraftment (Sakai et al., 2003; Singh et al., 2009) were due predominantly, if not exclusively, to altered homing of HSCs from TCDD-treated animals. Alterations in the expression and/or function of CD184/CXCR4 and CD44 on these cells are probably concomitant with functional changes. Because the AhR is a transcription factor, we hypothesized that the phenotypic and cellular changes observed above were the consequence of AhR-mediated changes in gene ex-

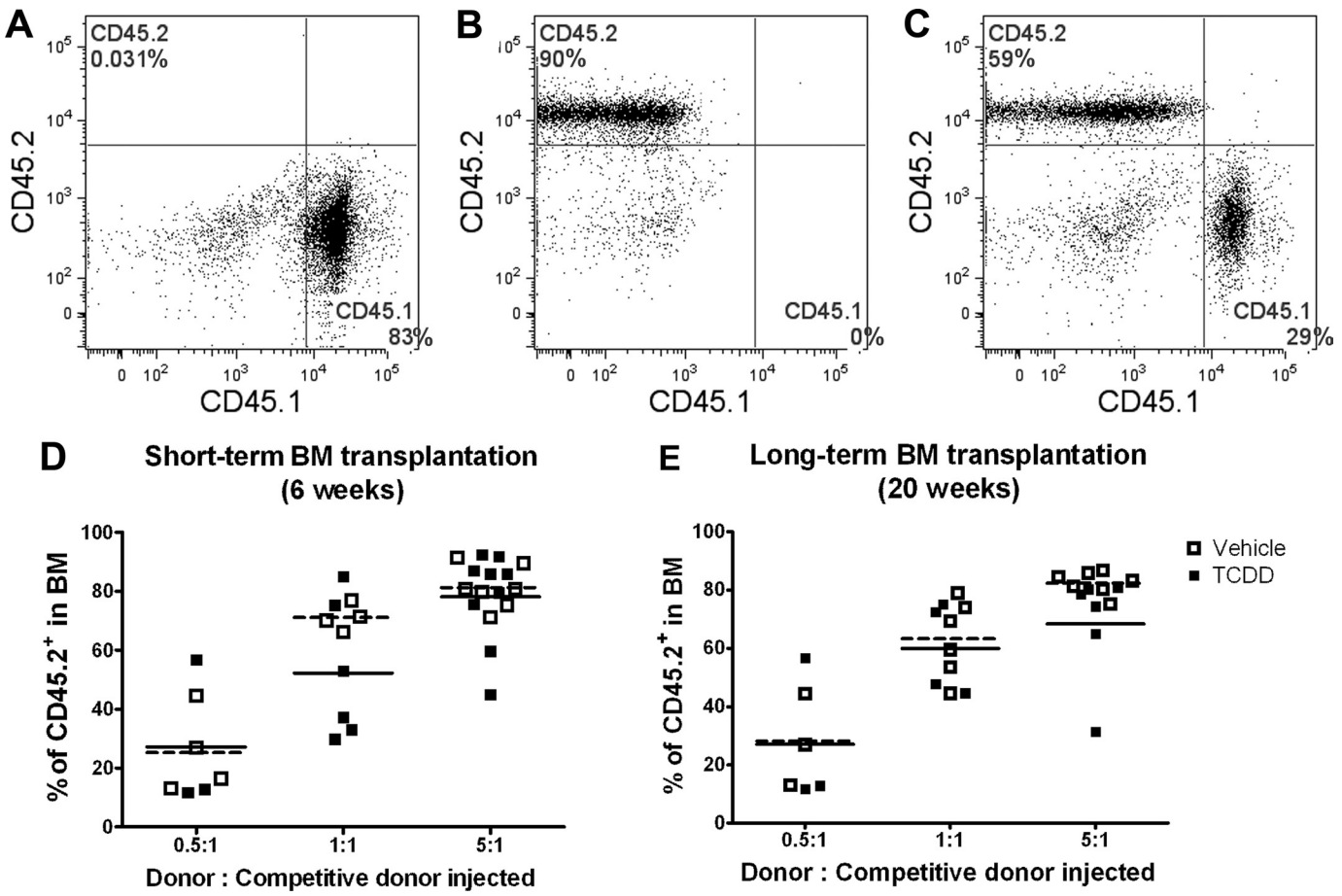

Fig. 2. Qualitative analysis of engrafted TCDD-treated BM cells shows no difference in the engraftment potential of HSCs. Donor CD45.2$^+$ BM cells from TCDD-treated (30 μg/kg, 7 days) mice were simultaneously injected with CD45.1$^+$ competitor BM cells at different ratios into CD45.1$^+$ irradiated recipient mice. Representative gating was applied for competitive donor BM cells (A) and (B) donor BM cells. After reconstitution, the long-term (20 weeks) and short-term (6 weeks) ability to reconstitute the BM was qualitatively analyzed. C, flow cytometry was used to discriminate CD45.2$^+$ donor cells from CD45.1$^+$ competitive donor cells in repopulated recipients. Cumulative data for the percentage of the donor's progeny (CD45.2$^+$) show no differences 6 (D) or 20 (E) weeks after transplantation. Data shown represent one independent experiment of two with eight recipients per group per experiment. Squares represent values for individual mice. Average values for vehicle and TCDD groups are represented by dashed and solid lines, respectively.

pression. Differential gene expression in LSK cells from mice treated with TCDD (30 μg/kg) or vehicle for 6 and 12 h was analyzed using microarray technology. Hierarchical clustering of the expression profiles showed that the most significant changes in regulation occurred for 105 transcripts (Fig. 4A). Transcripts consistently up-regulated at 6 and 12 h included Scinderin (*Scin*), *Mmp8*, interleukin 1 family member 9 (*Il1f9*), NAD(P)H dehydrogenase quinone 1 (*Nqo1*), Filamin beta (*Flnb*), mouse predicted gene *Gm5662*, and SLAM family member 7 (*Slamf7*) (Table 2). The lists of up- or down-regulated transcripts at 6 and 12 h can be found in Supplemental Tables 2, 3, and 4. Results from RT^2-PCR analyses (Fig. 4, B and C) validate the changes observed at 6 and 12 h. There were some notable differences between the responses at 6 and 12 h. At 6 h, several genes (*Olfr1095*, *Mmp9*, *Ceacam10*, *Retnig*, *Msr1*, and *Lcn2*) were up-regulated >2-fold but demonstrated no significant change at 12 h (Fig. 4A; Supplemental Table 2). In contrast, other genes, including *Fosb*, *Cxcl2*, *Egr1*, *Atf3*, *Nr4a1*, *Fos*, *Jun*, *Junb*, *Dusp1*, *Plk2*, *Ptgs2* (*Cox2*), *Cd69*, *Ighg*, *Slc10a1*, and *Myd116*, were down-regulated at 6 h but were significantly up-regulated (*Cxcl2*, *Nr4a1*, *Plk2*, *Ptgs2*, and *Cd69*) or not altered at 12 h (Fig. 4A; Supplemental Tables 3 and 4).

To understand the biological relevance of the observed changes, IPA was used to generate functional association networks with the following settings: direct relationships from the Ingenuity Knowledge Base Reference Set reported in all human, mouse, and rat immune primary cells and immune, leukemia, lymphoma, macrophage, and myeloma cell lines; cutoff fold change values 1.5; up to 25 networks per analysis; and up to 35 molecules per network. Table 3 shows that the common top biological functions at 6 and 12 h were cell-to-cell signaling and interaction and cellular movement. In addition, at these time points, hematological system development and function were significantly affected by treatment. Supplemental Tables 5 and 6 show the detailed lists of transcripts assigned by IPA to the most relevant molecular and cellular functions and physiological systems and functions. It is noteworthy that changes in genes involved in the biological functions of antigen presentation, cell-to-cell signaling and interaction, cellular movement, hematological system development and function, and immune cell trafficking appeared to be most significant (defined by $p < 10^{-7}$) in the 12-h response to TCDD (Table 3). Figure 5 shows functional association networks of transcripts assigned to hematological system development and function, generated by IPA

TABLE 1

Quantitative analysis of engrafted TCDD-treated BM cells shows no difference in the engraftment potential of HSCs

Donor BM cells were harvested from mice 7 days after treatment with TCDD (30 μg/kg) or vehicle (olive oil) by gavage as described in the legend to Fig. 2. Repopulated recipients contained >1% of CD45.2$^+$ cells in total BM cells. The proportions of HSCs per million of BM cells were calculated using L-Calc software, entering the numbers of total surviving and repopulated mice. Representative results from one of two independent experiments (n = 8 recipients per dilution of donor BM cells/group). A Pearson χ^2 p value = 1 was consistent with a Poisson distribution of data.

	Short-Term (6 weeks)		Long-Term (20 weeks)	
	Vehicle	TCDD	Vehicle	TCDD
Proportion (HSCs per 10^6 BM cells)	13.4	11.0	10.3	6.1
95% confidence interval	6.0–30	5.3–22	5.1–21	2.9–13
p value for Pearson χ^2	0.7966	0.4722	0.9853	0.9507

at 6 and 12 h. An analysis was also run using information reported from hematopoietic and nonhematopoietic cells. According to this analysis, the top biological functions and diseases associated with the network generated by the molecular interactions common to both time points were gene expression (RNA polymerase II, histone h3, and histone h4), inflammation (*Ptgs2*, also known as *Cox2* and NF-κB complex), and cancer (*Ptgs2*, *Cxcl2*, *Jun*, *Fos*, *Atf3*, *Mmp9*, *Nqo1*, *Nr4a1*, *Cd69*, *Btg2*, *Egr1*, and *Dusp1*).

Discussion

There is increasing evidence supporting a role of the AhR in hematopoiesis and HSC biology in particular. In part, this evidence comes from reports of increased incidence of leukemia and non-Hodgkin's lymphoma in TCDD-exposed populations (Frumkin 2003) as well as recent studies suggesting a potential therapeutic application of AhR antagonists to expand human HSCs for BM transplants (Boitano et al., 2010). Thus, there is a need to define cellular and molecular mechanisms whereby the AhR mediates these effects.

It has been shown that TCDD exposure to mice increases the percentages of LSK cells and some LSK subpopulations in BM (Sakai et al., 2003; Singh et al., 2009). Here we expand on these reports by showing that the percentage of

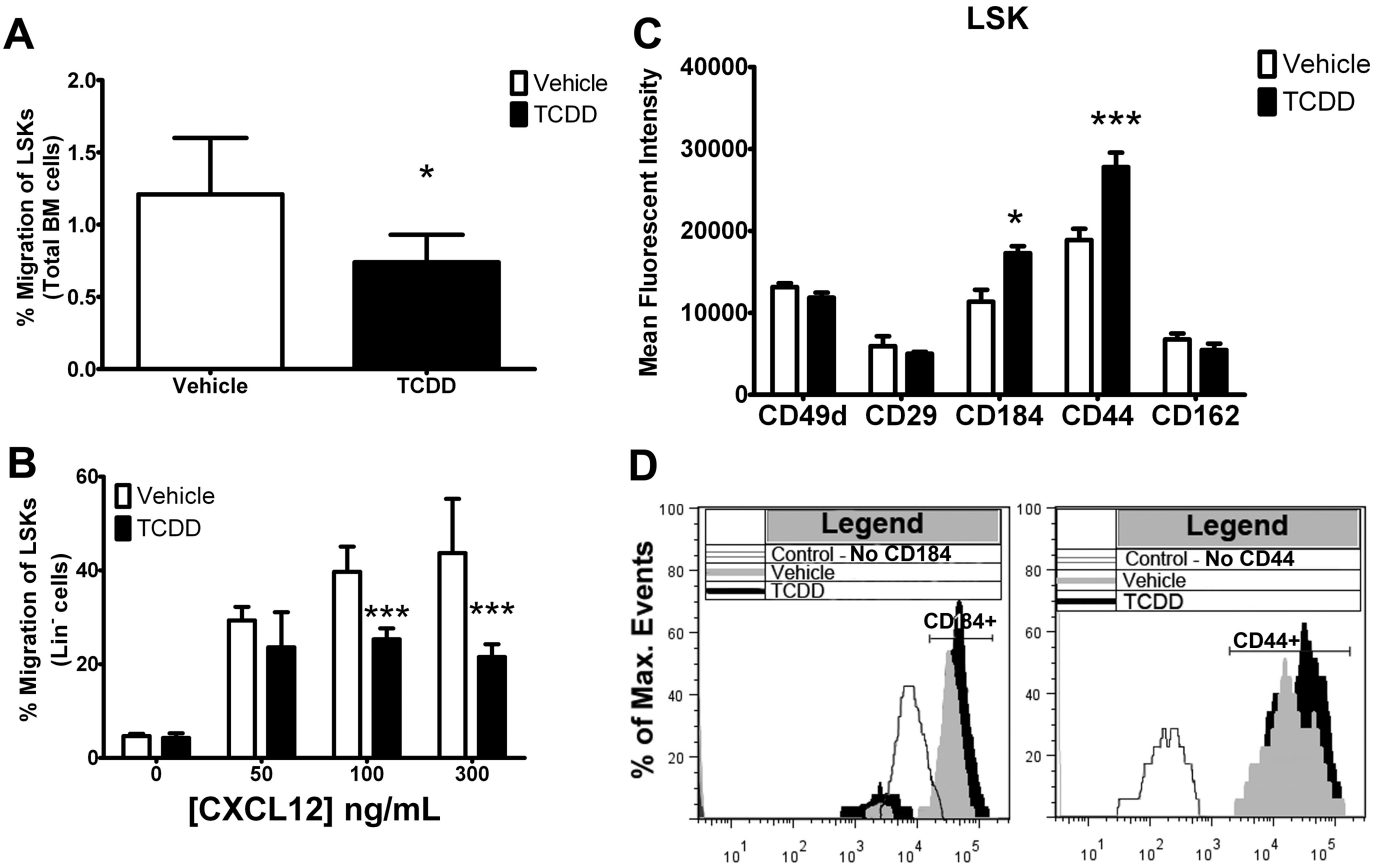

Fig. 3. TCDD exposure altered the migration of HSCs in vivo and in vitro. BM cells were harvested from mice treated with TCDD (30 μg/kg, 7 days) or vehicle. A, five million CD45.2$^+$ BM cells from TCDD-treated or untreated mice were injected intravenously into CD45.1$^+$ recipients. After 24 h, flow cytometry was used to determine the numbers of donor LSK cells that migrated to BM in recipients with respect to the LSK numbers injected. (p = 0.0242). Error bars are S.E.M of n = 3 independent experiments using data from five to six individual mice per experiment. B, 500,000 Lin$^-$ cells were placed on top of a transwell migration chamber containing 50 to 300 ng/ml CXCL12 in the bottom chamber. Three hours later, LSK cells that migrated to the bottom chamber were counted by flow cytometry. Two-way ANOVA analysis indicated significant differences at 100 and 300 ng/ml (p < 0.0001). Error bars are S.E.M. of n = 3 independent experiments using data from 12 wells with cells from three pooled mice. C, LSK cells were analyzed for expression of surface molecules by flow cytometry. Two-way ANOVA analysis indicated significant differences between groups for CD184/CXCR4 and CD44 (p = 0.0037 and <0.0001, respectively). Error bars are S.E.M. of n = 3 independent experiments using data from five to six individual mice. D, representative histograms obtained using flow cytometry to determine the mean fluorescent intensity of CD184/CXCR4 and CD44 in viable LSK cells. The filled histograms are representative of TCDD-treated (black) and vehicle-treated (gray) cells. The unfilled histograms are representative of the negative controls used to compensate for fluorescent signals that were stained with all of the fluorochromes used in the respective panels except with the one conjugated to the protein being analyzed (CD184 or CD44). The horizontal bars represent the gating used to determine the positive population of cells for which the mean fluorescent intensity was calculated. *, p < 0.05; ***, p < 0.0001.

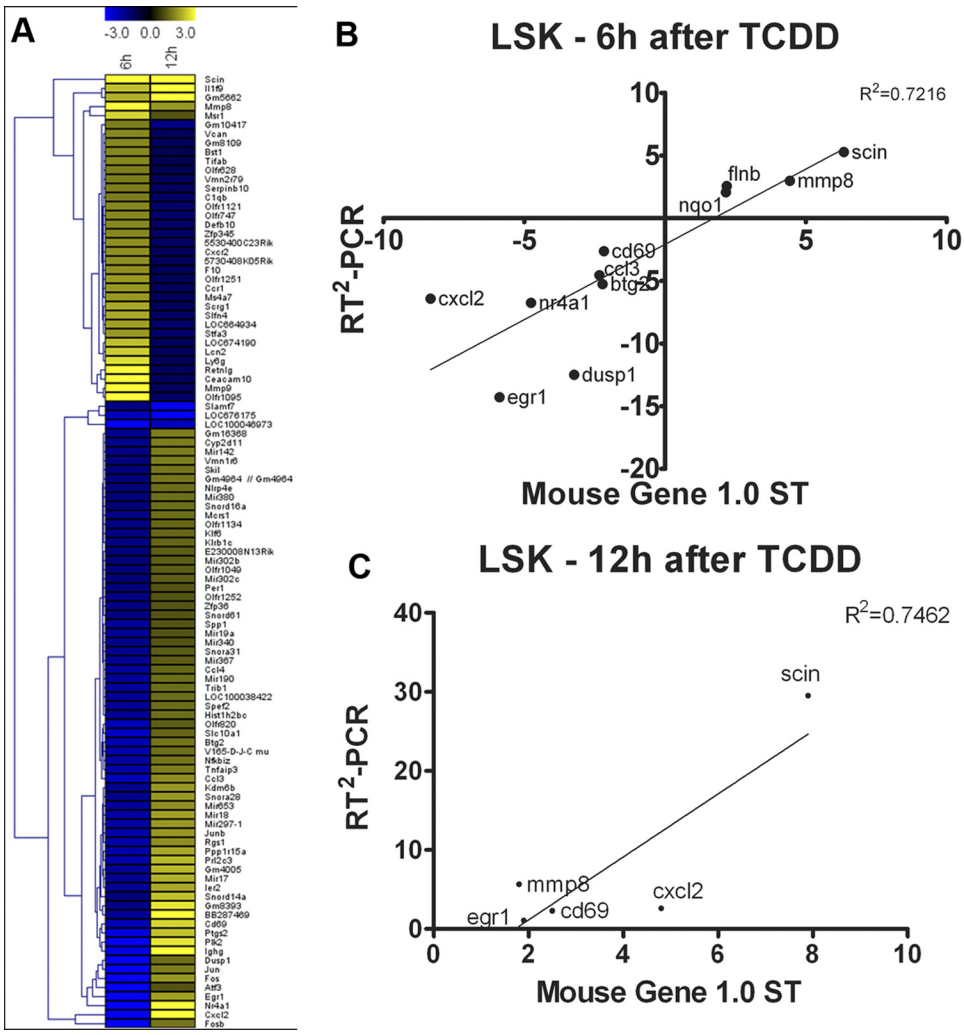

Fig. 4. TCDD exposure-induced changes in the expression of genes in LSK cells. Total RNA was obtained from sorted LSK cells. Fold changes in normalized values of gene expression for TCDD or vehicle control groups were calculated using microarray technology. Microarray data represent averages of five experiments using RNA from LSK cells pooled from 20 mice per treatment. A, the most variable transcripts from the 6- and 12-h data sets (fold change >1.5) were visualized using the Multi-experiment Viewer. The intensity of the colors represents the changes in fold change for the up-regulation (yellow) or down-regulation (blue) of the transcripts. Genes with significant fold changes in expression were used to validate microarray results using RT^2-PCR after 6 (B) and 12 h (C) of treatment. RT^2-PCR data are averages of three experiments from LSK cells pooled from 20 mice.

TABLE 2

Transcripts consistently up- or down-regulated at 6 h and 12 h in LSK cells after TCDD treatment

Microarray experiments were performed from LSK cells isolated using immunomagnetic sorting. Hierarchical clustering of microarray results was used to determine groups of genes coregulated. (n = 5 microarrays from pooled samples of 20 mice/group).

Gene Symbol	mRNA Accession Number	Fold Change (TCDD/Vehicle)	
		6 h	12 h
Scin	NM_001146196	6.4	7.9
Mmp8	NM_008611	4.4	1.8
Il1f9	NM_153511	2.3	4.3
Nqo1	NM_008706	2.2	1.6
Flnb	NM_134080	2.2	1.9
Gm5662	NM_001013824	2.1	3.9
Slamf7	NM_144539	−1.6	−3.2

$LSKCD48^{-}CD150^{-}$ and $LSKCD48^{-}CD150^{+}$ stem cells, identified by the recently described SLAM markers (Kiel et al., 2005), are also increased after TCDD treatment (Fig. 1). These results present the apparent paradox that higher percentages of phenotypically defined HSCs (LSK cells) occurred with a decreased functional ability of these cells to generate progeny (Sakai et al., 2003; Singh et al., 2009). This result may not necessarily be contradictory because it has been reported that when homeostasis is disrupted, cells with the phenotype of HSCs may have an altered functional capacity (Purton and Scadden, 2007). To avoid potential biases inherent with phenotypic-based sorting and defined relative ratios of donor to competitor cell numbers, we used a limiting dilution approach to quantify the functional integrity of these cells. These studies indicated no significant differences in the absolute proportions of long-term and short-term HSCs from TCDD- and vehicle-treated mice (Table 1). Together, these data suggested that the higher percentages of phenotypically defined HSCs reflected changes in HSC biology and cell signaling that may affect different steps of the engraftment process.

Successful engraftment of HSCs involves a number of different events such as leaving the circulation to home to the BM, taking residence in the vascular and endosteal niches, and finally lineage differentiation. Our studies further demonstrated that TCDD-mediated activation of the AhR alters the migration and trafficking of phenotypically defined HSCs under in vivo and in vitro conditions (Fig. 3, A and B). Thus, previously observed decreased engraftment (Sakai et al., 2003; Singh et al., 2009) is probably due to decreased migration (Fig. 3) rather than to decreased numbers of functional HSCs (Fig. 2; Table 1) or altered viability and differentiation (Supplemental Figs. 1 and 2). A modified ability of HSCs and progenitors to move within the marrow niche may also explain the effects of AhR activation by TCDD on more differentiated cells [i.e., decreased thymic

TABLE 3

Important biological functions were significantly altered in LSK cells 6 and 12 h after TCDD treatment

A cutoff of 1.5-fold change (TCDD/vehicle) was set to identify transcripts whose expression was regulated. The top biological functions based on their Fisher's exact test *p* value (in brackets) are shown. The numbers in parentheses after the name of the functions are the number of transcripts in our data sets common to the Ingenuity Knowledge Base reference set.

	6 h	12 h
Molecular and cellular functions	Cell-to-cell signaling and interaction (23) [9.52×10^{-4}–3.92×10^{-2}] Cellular movement (9) [2.20×10^{-3}–4.48×10^{-2}] Antigen presentation (16) [2.51×10^{-3}–3.92×10^{-2}] Cellular development (19) [4.54×10^{-3}–4.31×10^{-2}] Cell morphology (4) [9.90×10^{-3}–2.67×10^{-2}]	Antigen presentation (17) [2.11×10^{-8}–4.44×10^{-2}] Cell-to-cell signaling and interaction (16) [2.11×10^{-8}–4.89×10^{-2}] Cellular movement (14) [1.54×10^{-7}–4.44×10^{-2}] Cell death (10) [3.65×10^{-6}–4.44×10^{-2}] Cell signaling (27) [9.02×10^{-6}–2.48×10^{-3}]
Physiological system development and function	Hematological system development and function (44) [2.79×10^{-5}–4.96×10^{-2}] Tissue morphology (17) [2.79×10^{-5}–2.67×10^{-2}] Lymphoid tissue structure and development (10) [1.39×10^{-3}–3.92×10^{-2}] Hematopoiesis (20) [2.20×10^{-3}–4.48×10^{-2}] Immune cell trafficking (23) [2.20×10^{-3}–4.96×10^{-2}]	Hematological system development and function (26) [2.11×10^{-8}–4.89×10^{-2}] Immune cell trafficking (17) [2.11×10^{-8}–4.89×10^{-2}] Hematopoiesis (15) [2.75×10^{-7}–4.44×10^{-2}] Lymphoid tissue structure and development (12) [6.22×10^{-5}–2.25×10^{-2}] Humoral immune response (3) [1.13×10^{-4}–2.98×10^{-2}]

seeding (Fine et al., 1990; Laiosa et al., 2010)] and altered B cell numbers (Thurmond et al., 2000).

Trafficking events are dependent on the ability of HSCs to "sense" their microenvironment by cell-cell interactions and the recognition of soluble factors through cell surface proteins. Markers used for phenotypic discrimination are functional molecules themselves involved in cell signaling through recognition of chemical cues from the microenvironment to migrate, differentiate, proliferate, or self-renew. For example, c-kit is a tyrosine kinase serving as a receptor of the stem cell factor, which provides cues for quiescence and survival of the most primitive progenitor cells in the BM (Askmyr et al., 2009). CD184/CXCR4 is critical during development for seeding of the BM with HSCs and mediates migration and quiescence throughout adulthood (Nie et al., 2008). CD44 is highly expressed in prothymocytes ($CD4^{low}CD25^{-}$c-kit^{+}) of the BM, serving as a homing receptor for the thymus (Wu et al., 1993), and CD44 expression was found to be up-regulated in thymic emigrants exposed to TCDD (Esser et al., 2004). Thus, it is reasonable, if not expected, that functional alterations in HSCs after TCDD treatment would be a reflection of altered expression and/or function of cell surface proteins. However, we observed an increased, rather than an expected decreased, phenotypic expression of both CD184/CXCR4 and CD44 at 7 days after TCDD treatment (Fig. 3). No differences were observed in CD184/CXCR4 or CD44 mRNA expression at 6 or 12 h after TCDD exposure as determined by the microarray data. In addition, CD184/CXCR4 mRNA expression at 24 h or 7 days after TCDD exposure was not changed as determined by RT^2-PCR analysis (not shown). Taken together, these data suggest that TCDD may cause altered CD184/CXCR4 and CD44 protein expression in HSCs by a post-transcriptional mechanism and that other molecules are being affected by AhR activation that either alter the function of these proteins or that are involved the migration and trafficking of these cells.

Given that the AhR is a ligand-activated transcription factor, we hypothesize that TCDD-mediated changes in phenotype and signaling of HSCs were preceded by changes in gene expression. The results shown in Figs. 4 and 5 support this hypothesis. Multiple transcriptional changes occurred 6 h after exposure, some of which were transient and other were also observed 6 h later. The genes modulated by AhR activation in LSK cells that have been reported to have putative AhR responsive elements (Sun et al., 2004) in the promoters of their murine homologs include *Scin*, *Nqo1*, *Egr1*, *Ptgs2*, *Cxcl2*, *Nr4a1*, *Dusp1*, *Btg2*, *Junb*, *Fosb*, *Jun*, *Ceacam10*, *Scrg1*, *C1qb*, *Bst1*, *Slc10a1*, *Spp1*, *Snord14a*, *Ier2*, *Ccl4*, *Skil*, and *Klrb1c*, although it is not yet clear whether all of these sites represent AhR responsive elements that are functional.

Scinderin (*Scin*, also known as adseverin) was highly up-regulated after both 6 and 12 h of TCDD treatment (Table 2). In hematopoietic stem and progenitor cells, *Scin* is one of the key regulators accounting for chemotactic responses to CXCL12 (Evans et al., 2004). This calcium/proton-regulated protein binds actin monomers, severs and caps actin filaments, and has been reported to respond to TCDD treatment in other immune cells (Svensson et al., 2002). Sequential coordinated polymerization and depolymerization of the actin cytoskeleton are necessary to maintain the functional expression of cell surface proteins and for directed migration (Friederich et al., 1992). CD184/CXCR4 function and cell surface expression is known to depend on endocytosis, intracellular trafficking, and recycling (Kumar et al., 2011), all of which are dependent on cytoskeleton regulation. $Lin^{-}Sca\text{-}1^{+}ckit^{-}$ and LSK cells move with different efficiencies toward CXCL12 due at least in part to different expression of Scin protein (Evans et al., 2004). Given that TCDD can regulate *Scin* transcripts and responses to CXCL12 in LSK cells, our results support a role for the AhR in cytoskeleton regulation that may have consequences for cell motility.

Mmp8 was also up-regulated at both time points. Even though there is no evidence of AhR transcriptionally regulating metalloproteinases, there is literature data linking AhR activation with their expression, probably via *Jun* or *Fos* (Hillegass et al., 2006). Together with CD184, metalloproteinases have been proposed to be involved in cell migration and invasion of leukemic cells (Shao et al., 2011). Different tran-

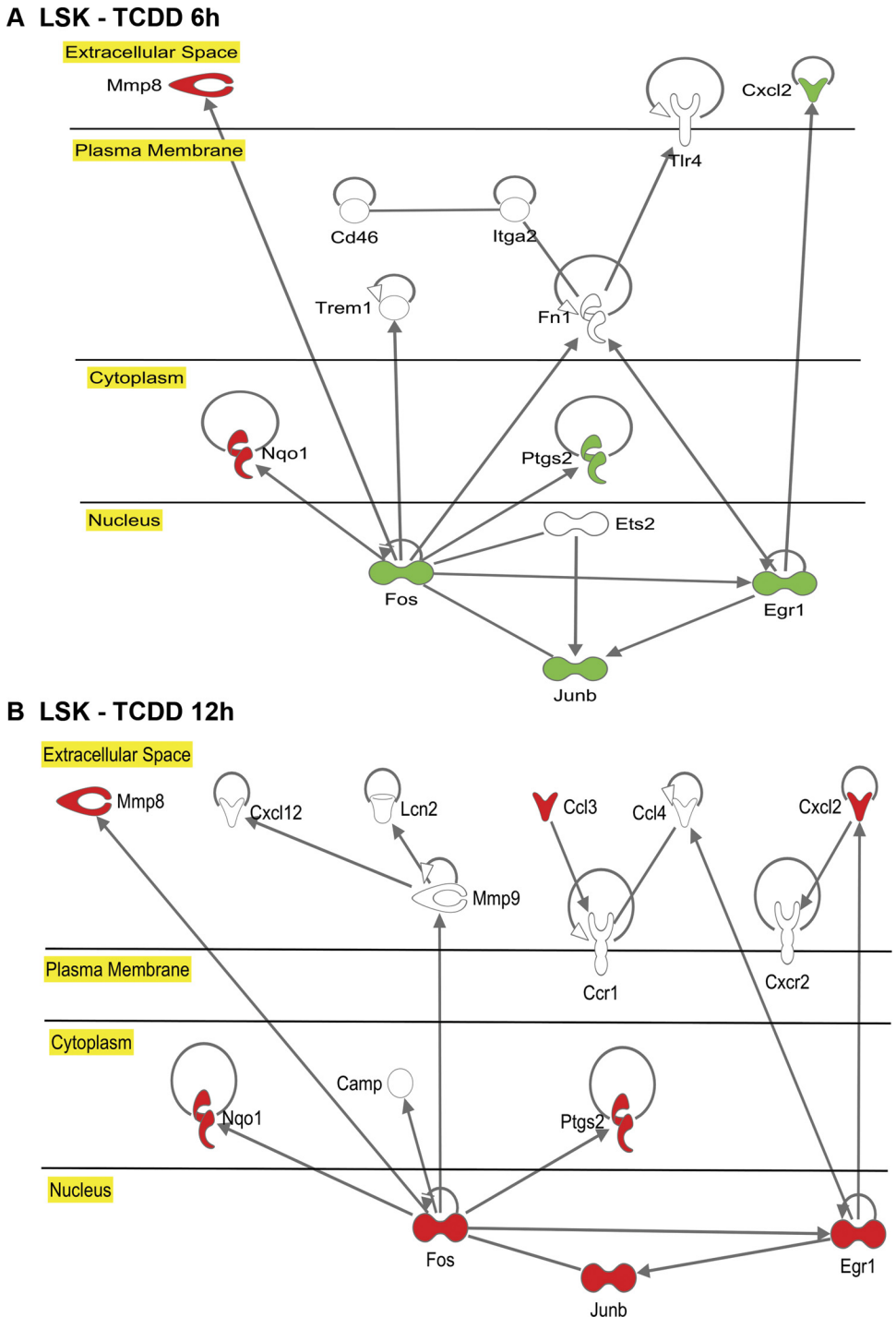

Fig. 5. TCDD treatment changes the expression of transcripts involved in hematopoietic system development and function. Data sets containing 35,556 microarray probes were analyzed at 6 and 12 h. Transcripts with regulated expression were overlaid onto a global molecular network developed from information contained in the Ingenuity Knowledge Base. All relationships are supported by at least one reference from the literature, from a textbook, or from canonical information stored in the Ingenuity Knowledge Base. Hematopoietic system development and function was regulated after TCDD treatment. Association networks of the transcripts regulated in this category after 6 (A) and 12 (B) h were generated using IPA. In the graphical representation of the molecular relationships, transcripts are represented as nodes with shapes indicating the function of the expressed protein. The color of the node indicates the up-regulation (red) or down-regulation (green) (fold changes >1.5) of the transcripts. The noncolor transcripts were present in our data set and have a direct relationship with the regulated transcripts. In addition, according to the Ingenuity Knowledge Base, these are categorized within hematopoietic system development and function.

scripts involved in NF-κB signaling such as *Il1f9*, *Cxcl2*, *Ptgs2*, *Junb*, and *Fos* (Table 2; Supplemental Table 3) were also altered at both time points. Whether these changes in gene expression are directly related to AhR-DNA binding in LSK cells is uncertain because there is evidence that AhR and NF-κB proteins can interact directly (Tian, 2009). Further kinetic studies to clarify these interactions are of therapeutic interest, considering that NF-κB complexes regulate CD184 (Chua et al., 2010) and CD44 (Damm et al., 2010) protein expression. It is also of interest that *Spp1* was down-regulated 6 h after TCDD exposure. *Spp1* encodes osteopontin, one of the ligands of CD44. The reduced expression of a CD44 ligand (Supplemental Table 4) at early time points may be related to increased CD44 expression (Fig. 3C) several days later. Given that some of the transcripts changed in our data sets are themselves transcriptional regulators and are regulated by the AhR (e.g., *Fos*, *JunB*, *Ptgs2*, and *Egr1*), it seems likely that some of the functional changes are secondary to initial AhR signaling. Although supporting the functional changes that we observed in hematopoietic stem/progenitor cells after TCDD treatment, the changes in gene expression also suggest a complex cross-talk of the AhR with pathways associated with the ability of HSCs to sense their microenvironment, alter their trafficking behavior, and pro-

mote hematological diseases, which is a common sequence of events in leukemogenesis.

Taken together, these results suggest a complex role of AhR signaling in HSC function. Additional studies in *AhR*-null mice suggest that AhR may regulate HSC quiescence/proliferation (Singh et al., 2010), which, consistent with the present study, depend on the ability of HSCs to sense cues within their microenvironment. It is also important to consider that the exact role of the AhR and its physiological relevance in other tissue stem cell populations may be context-specific (Panteleyev and Bickers, 2006; Latchney et al., 2011). Clinical use of the AhR to treat hematological diseases (Boitano et al., 2010; Quintana et al., 2010) will also require answering daunting questions regarding the biological implications of different, and possibly endogenous, ligands in AhR activity and the relevance of nongenomic pathways in AhR signaling. Nevertheless, further investigations in this area will provide important information needed for our understanding of processes that regulate stem cells and their role in human disease.

Acknowledgments

We thank Dr. Ellen Henry for critical discussion and reading of the manuscript, Jason Walrath for assistance with animal care, Dr. Timothy Bushnell and the staff of the Flow Core Facilities in URMC and Dr. Stephen Welle and the staff of the Functional Genomics Core of the URMC.

Authorship Contributions

Participated in research design: Casado, Singh, and Gasiewicz.
Conducted experiments: Casado and Singh.
Performed data analysis: Casado, Singh, and Gasiewicz.
Wrote or contributed to the writing of the manuscript: Casado, Singh, and Gasiewicz.
Other:

References

Askmyr M, Sims NA, Martin TJ, and Purton LE (2009) What is the true nature of the osteoblastic hematopoietic stem cell niche? *Trends Endocrinol Metab* **20:**303–309.
Boitano AE, Wang J, Romeo R, Bouchez LC, Parker AE, Sutton SE, Walker JR, Flaveny CA, Perdew GH, Denison MS, et al. (2010) Aryl hydrocarbon receptor antagonists promote the expansion of human hematopoietic stem cells. *Science* **329:**1345–1348.
Chua AW, Hay HS, Rajendran P, Shanmugam MK, Li F, Bist P, Koay ES, Lim LH, Kumar AP, and Sethi G (2010) Butein downregulates chemokine receptor CXCR4 expression and function through suppression of NF-κB activation in breast and pancreatic tumor cells. *Biochem Pharmacol* **80:**1553–1562.
Damm S, Koefinger P, Stefan M, Wels C, Mehes G, Richtig E, Kerl H, Otte M, and Schaider H (2010) HGF-promoted motility in primary human melanocytes depends on CD44v6 regulated via NF-κB, Egr-1, and C/EBP-β. *J Invest Dermatol* **130:**1893–1903.
Esser C, Temchura V, Majora M, Hundeiker C, Schwärzler C, and Günthert U (2004) Signaling via the AHR leads to enhanced usage of CD44v10 by murine fetal thymic emigrants: possible role for CD44 in emigration. *Int Immunopharmacol* **4:**805–818.
Evans CA, Tonge R, Blinco D, Pierce A, Shaw J, Lu Y, Hamzah HG, Gray A, Downes CP, Gaskell SJ, et al. (2004) Comparative proteomics of primitive hematopoietic cell populations reveals differences in expression of proteins regulating motility. *Blood* **103:**3751–3759.
Fine JS, Silverstone AE, and Gasiewicz TA (1990) Impairment of prothymocyte activity by 2,3,7,8-tetrachlorodibenzo-p-dioxin. *J Immunol* **144:**1169–1176.
Frericks M, Meissner M, and Esser C (2007) Microarray analysis of the AHR system: tissue-specific flexibility in signal and target genes. *Toxicol Appl Pharmacol* **220:**320–332.
Friederich E, Vancompernolle K, Huet C, Goethals M, Finidori J, Vandekerckhove J, and Louvard D (1992) An actin-binding site containing a conserved motif of charged amino acid residues is essential for the morphogenic effect of villin. *Cell* **70:**81–92.
Frumkin H (2003) Agent Orange and cancer: an overview for clinicians. *CA Cancer J Clin* **53:**245–255.
Henry EC, Welle SL, and Gasiewicz TA (2010) TCDD and a putative endogenous AhR ligand, ITE, elicit the same immediate changes in gene expression in mouse lung fibroblasts. *Toxicol Sci* **114:**90–100.
Hillegass JM, Murphy KA, Villano CM, and White LA (2006) The impact of aryl hydrocarbon receptor signaling on matrix metabolism: implications for development and disease. *Biol Chem* **387:**1159–1173.
Kiel MJ, Yilmaz OH, Iwashita T, Yilmaz OH, Terhorst C, and Morrison SJ (2005) SLAM family receptors distinguish hematopoietic stem and progenitor cells and reveal endothelial niches for stem cells. *Cell* **121:**1109–1121.
Kremer J, Gleichmann E, and Esser C (1994) Thymic stroma exposed to arylhydrocarbon receptor-binding xenobiotics fails to support proliferation of early thymocytes but induces differentiation. *J Immunol* **153:**2778–2786.
Kumar A, Kremer KN, Dominguez D, Tadi M, and Hedin KE (2011) Gα13 and Rho mediate endosomal trafficking of CXCR4 into Rab11$^+$ vesicles upon stromal cell-derived factor-1 stimulation. *J Immunol* **186:**951–958.
Laiosa MD, Mills JH, Lai ZW, Singh KP, Middleton FA, Gasiewicz TA, and Silverstone AE (2010) Identification of stage-specific gene modulation during early thymocyte development by whole-genome profiling analysis after aryl hydrocarbon receptor activation. *Mol Pharmacol* **77:**773–783.
Latchney SE, Lioy DT, Henry EC, Gasiewicz TA, Strathmann FG, Mayer-Pröschel M, and Opanashuk LA (2010) Neural precursor cell proliferation is disrupted through activation of the aryl hydrocarbon receptor by 2,3,7,8-tetrachlorodibenzo-*p*-dioxin. *Stem Cells Dev* **20:**313–326.
Murante FG and Gasiewicz TA (2000) Hemopoietic progenitor cells are sensitive targets of 2,3,7,8-tetrachlorodibenzo-*p*-dioxin in C57BL/6J mice. *Toxicol Sci* **54:**374–383.
Mustafa A, Holladay SD, Goff M, Witonsky SG, Kerr R, Reilly CM, Sponenberg DP, and Gogal RM Jr (2008) An enhanced postnatal autoimmune profile in 24 week-old C57BL/6 mice developmentally exposed to TCDD. *Toxicol Appl Pharmacol* **232:**51–59.
Nie Y, Han YC, and Zou YR (2008) CXCR4 is required for the quiescence of primitive hematopoietic cells. *J Exp Med* **205:**777–783.
Panteleyev AA and Bickers DR (2006) Dioxin-induced chloracne–reconstructing the cellular and molecular mechanisms of a classic environmental disease. *Exp Dermatol* **15:**705–730.
Poland A and Glover E (1973) Studies on the mechanism of toxicity of the chlorinated dibenzo-p-dioxins. *Environ Health Perspect* **5:**245–251.
Purton LE and Scadden DT (2007) Limiting factors in murine hematopoietic stem cell assays. *Cell Stem Cell* **1:**263–270.
Quintana FJ, Murugaiyan G, Farez MF, Mitsdoerffer M, Tukpah AM, Burns EJ, and Weiner HL (2010) An endogenous aryl hydrocarbon receptor ligand acts on dendritic cells and T cells to suppress experimental autoimmune encephalomyelitis. *Proc Natl Acad Sci USA* **107:**20768–20773.
Saeed AI, Sharov V, White J, Li J, Liang W, Bhagabati N, Braisted J, Klapa M, Currier T, Thiagarajan M, et al. (2003) TM4: a free, open-source system for microarray data management and analysis. *BioTechniques* **34:**374–378.
Sakai R, Kajiume T, Inoue H, Kanno R, Miyazaki M, Ninomiya Y, and Kanno M (2003) TCDD treatment eliminates the long-term reconstitution activity of hematopoietic stem cells. *Toxicol Sci* **72:**84–91.
Sasaki Y, Matsuoka Y, Hase M, Toyohara T, Murakami M, Takahashi M, Nakatsuka R, Uemura Y, and Sonoda Y (2009) Marginal expression of CXCR4 on c-kit(+)Sca-1(+)Lineage (−) hematopoietic stem/progenitor cells. *Int J Hematol* **90:**553–560.
Shao HY, Miao ZY, Hui-Chen, Qin FX, Chen XC, Tan S, Zhang HJ, Wang L, Gao YJ, Yang ZL, and Zhang L (2011) Nucleophosmin gene mutations promote NIH3T3 cell migration and invasion through CXCR4 and MMPs. *Exp Mol Pathol* **90:**38–44.
Singh KP, Garrett RW, Casado FL, and Gasiewicz TA (2011) Aryl hydrocarbon receptor-null allele mice have hematopoietic stem/progenitor cells with abnormal characteristics and functions. *Stem Cells Dev* **20:**769–784.
Singh KP, Wyman A, Casado FL, Garrett RW, and Gasiewicz TA (2009) Treatment of mice with the Ah receptor agonist and human carcinogen dioxin results in altered numbers and function of hematopoietic stem cells. *Carcinogenesis* **30:**11–19.
Soshilov A and Denison MS (2008) Role of the Per/Arnt/Sim domains in ligand-dependent transformation of the aryl hydrocarbon receptor. *J Biol Chem* **283:**32995–33005.
Staples JE, Murante FG, Fiore NC, Gasiewicz TA, and Silverstone AE (1998) Thymic alterations induced by 2,3,7,8-tetrachlorodibenzo-p-dioxin are strictly dependent on aryl hydrocarbon receptor activation in hemopoietic cells. *J Immunol* **160:**3844–3854.
Stevens EA, Mezrich JD, and Bradfield CA (2009) The aryl hydrocarbon receptor: a perspective on potential roles in the immune system. *Immunology* **127:**299–311.
Sun YV, Boverhof DR, Burgoon LD, Fielden MR, and Zacharewski TR (2004) Comparative analysis of dioxin response elements in human, mouse and rat genomic sequences. *Nucleic Acids Res* **32:**4512–4523.
Svensson C, Silverstone AE, Lai ZW, and Lundberg K (2002) Dioxin-induced adseverin expression in the mouse thymus is strictly regulated and dependent on the aryl hydrocarbon receptor. *Biochem Biophys Res Commun* **291:**1194–1200.
Thurmond TS, Staples JE, Silverstone AE, and Gasiewicz TA (2000) The aryl hydrocarbon receptor has a role in the in vivo maturation of murine bone marrow B lymphocytes and their response to 2,3,7,8-tetrachlorodibenzo-p-dioxin. *Toxicol Appl Pharmacol* **165:**227–236.
Tian Y (2009) Ah receptor and NF-κB interplay on the stage of epigenome. *Biochem Pharmacol* **77:**670–680.
Wilson A, Laurenti E, Oser G, van der Wath RC, Blanco-Bose W, Jaworski M, Offner S, Dunant CF, Eshkind L, Bockamp E, et al. (2008) Hematopoietic stem cells reversibly switch from dormancy to self-renewal during homeostasis and repair. *Cell* **135:**1118–1129.
Wu L, Kincade PW, and Shortman K (1993) The CD44 expressed on the earliest intrathymic precursor population functions as a thymus homing molecule but does not bind to hyaluronate. *Immunol Lett* **38:**69–75.

Address correspondence to: Dr. Thomas A. Gasiewicz, Department of Environmental Medicine, University of Rochester, School of Medicine and Dentistry, Box-EHSC, 601 Elmwood Ave., Rochester, NY 14642. E-mail: tom_gasiewicz@urmc.rochester.edu